atmosphere

Article

Mobile Measurements of Atmospheric Methane at Eight Large Landfills: An Assessment of Temporal and Spatial Variability

Tian Xia [1,*], Sachraa G. Borjigin [1], Julia Raneses [1], Craig A. Stroud [2] and Stuart A. Batterman [1]

[1] Department of Environmental Health Sciences, School of Public Health, University of Michigan, M6075 SPH II, 1415 Washington Heights, Ann Arbor, MI 48109, USA; sachraa@umich.edu (S.G.B.); stuartb@umich.edu (S.A.B.)

[2] Air Quality Research Division, Environment and Climate Change Canada (ECCC), 4905 Dufferin Street, Toronto, ON M3H 5T4, Canada; craig.stroud@ec.gc.ca

* Correspondence: xiatian@umich.edu

Abstract: Municipal solid waste landfills are major contributors to anthropogenic emissions of methane (CH_4), which is the major component of natural gas, a potent greenhouse gas, and a precursor for the formation of tropospheric ozone. The development of sensitive, selective, and fast-response instrumentation allows the deployment of mobile measurement platforms for CH_4 measurements at landfills. The objectives of this study are to use mobile monitoring to measure ambient levels of CH_4 at eight large operating landfills in southeast Michigan, USA; to characterize diurnal, daily and spatial variation in CH_4 levels; and to demonstrate the influence of meteorological factors. Elevated CH_4 levels were typically found along the downwind side or corner of the landfill. Levels peaked in the morning, reaching 38 ppm, and dropped to near-baseline levels during midday. Repeat visits showed that concentrations were highly variable. Some variation was attributable to the landfill size, but both mechanistically-based dilution-type models and multivariate models identified that wind speed, boundary layer height, barometric pressure changes, and landfill temperature were key determinants of CH_4 levels. Collectively, these four factors explained most (r^2 = 0.89) of the variation in the maximum CH_4 levels at the landfill visited most frequently. The study demonstrates the ability to assess spatial and temporal variation in CH_4 levels at landfills using mobile monitoring along perimeter roads. Such monitoring can identify the location of leaks and the best locations for long-term emission monitoring using fixed site monitors.

Keywords: methane; boundary layer; fugitive emissions; landfill gas; mobile monitoring; bootstrapping

check for updates

Citation: Xia, T.; Borjigin, S.G.; Raneses, J.; Stroud, C.A.; Batterman, S.A. Mobile Measurements of Atmospheric Methane at Eight Large Landfills: An Assessment of Temporal and Spatial Variability. *Atmosphere* **2023**, *14*, 906. https://doi.org/10.3390/atmos14060906

Academic Editor: James Lee

Received: 7 April 2023
Revised: 11 May 2023
Accepted: 12 May 2023
Published: 23 May 2023

1. Introduction

Methane (CH_4) is the second most important greenhouse gas (GHG) directly due to anthropogenic activities following carbon dioxide [1] and a precursor of tropospheric ozone, especially in unpolluted atmospheres [2]. Reducing CH_4 emissions can help to lower radiative forcing that warms the climate and can also decrease ozone pollution that causes adverse health impacts such as premature human mortality [3,4]. The three major sources of anthropogenic CH_4 emissions—the oil and gas industry, agriculture (e.g., enteric fermentation) and waste management (e.g., municipal solid waste (MSW) landfills) [5]—respectively, emit 27, 25 and 17% of anthropogenic CH_4 releases in the US, which are estimated to total 25,980 kilotons in 2021 [6–8]. Attention to CH_4 emissions has increased greatly. In particular, the rapid increase in the global atmospheric concentration of CH_4, increasing by 0.5%/year from 1.80 to 1.90 ppm in the past 10 years (2011–2021) [9] and the high social cost of CH_4 emissions, ranging from 1600 USD to 2200 USD/ton-year (2023–2035, 3% discount rate) [10], highlight the importance of identifying and controlling CH_4 releases at landfills and other sources. While the US Environmental Protection Agency (EPA) has regulated emission from larger landfills since 1996 [11], and landfill gas (LFG) collection, processing and reuse technologies have been widely adopted, the scale and nature of landfills pose challenges to LFG collection and control. LFG emissions at landfills occur as point, area and fugitive releases, e.g., at open cells prior to capping, through and around landfill caps and liners, gas collection networks, pumps, flares and other collection and treatment components.

MSW disposed in a landfill first undergoes aerobic decomposition, and typically within a year, anaerobic decomposition by methanogens becomes dominant. The composition and production rate of LFG, of which CH_4 typically accounts for 40–60% (by volume), tends to stabilize over time and remain relatively constant for over 20 years [6,12]. However, many factors can affect LFG emissions. A recent analysis of over U.S. 850 landfills estimated that gas collection systems at closed landfills achieved control efficiencies above 80%, while open or operating landfills had efficiencies below 70%, and noted that 91% of landfill CH_4 emissions occurred from open landfills [13]. Information regarding LFG emissions and control efficiencies is limited, and additional data, better monitoring approaches, and more robust models and assessments are needed to monitor and enforce CH_4 mitigation actions.

Ambient CH_4 measurements play an important role in estimating LFG emissions and impacts. From small to large scale, emissions can be estimated using surface flux chambers, eddy covariance, stationary mass balance, radial plume mapping, tracer gas dispersion, differential absorption LiDAR (DIAL), inverse modeling [14,15], and space observations using methane-tracking satellites such as MethaneSAT [16]. These methods have different strengths and limitations, including their ability to isolate and quantify specific locations where releases are occurring, to assess the temporal (diurnal and seasonal) variation in concentrations and emissions, and to provide representative and accurate measurements. The relatively recent availability of sensitive, selective, and fast-response instrumentation using cavity ring-down spectroscopy [17] and tunable diode laser absorption spectroscopy (TDLAS) [18] has allowed the use of mobile platforms for monitoring and mapping plumes of CH_4 and other pollutants at landfills and other sources. Advances in both unmanned aerial vehicles (UAV) and small and low-cost sensors [19], along with spatial interpolation algorithms [20], allow the ability to capture both horizontal and vertical CH_4 profiles. These data can be used to quantify emissions directly as fluxes, and indirectly using inverse dispersion modeling, although uncertainties may be high [21–23]. Compared with UAVs, on-road vehicle platforms can be equipped with larger, faster responding, and more accurate instruments, and sampling logistics are much easier, allowing repeated visits in most any kind of weather and time of day, but sampling is restricted to low measurement heights and often to perimeter roads around landfills. To date, vehicle-based mobile monitoring has been used to characterize regional sources of CH_4 where landfills were only considered as one of the sources [24–26]. Few studies have collected repeated measurements at landfills needed to evaluate effects of meteorological conditions and other factors that may affect the spatial and temporal variation of CH_4 levels at landfills.

The goal of this study is to characterize diurnal, daily and spatial variation of ambient CH_4 levels at large and operating landfills. We also evaluate the influence of meteorological conditions on CH_4 levels. The study uses extensive field data collected by the Michigan Pollution Assessment Laboratory (MPAL), a mobile laboratory equipped with sensitive CH_4 instruments, collected during repeated visits to eight landfills in southeast Michigan during the Michigan Ontario Oxidant Experience (MOOSE), an international field study investigating ozone precursors and potential controls. The study is also motivated by the number of large landfills around Detroit, which is currently classified as a non-attainment area for the ozone National Ambient Air Quality Standard, and by Michigan's top rank among U.S. states in terms of landfill waste disposed per person (66.5 tons/year) [27].

The study is novel as it is among the first to collect repeated measurements at all major landfills in a large urban area. Further, we characterize diurnal, daily and spatial variability in CH_4 levels, and evaluate the influence of meteorological conditions on concentrations. The study results can be used to help identify sources of landfill emissions, derive emission measurements, and inform ozone modeling and control strategies. We conclude with recommendations for future fixed-site and vehicle-based landfill CH_4 studies.

2. Materials and Methods

2.1. Landfill Visits

Eight operating landfills in southeast Michigan were visited in two phases. Figure S1 shows locations of the eight landfills, as well as CH_4 sources that exceed 0.5 ton/year in the study area. Each landfill has estimated CH_4 emissions that exceed 1000 ton/year; other CH_4 sources near the landfills are small [28]. Phase 1 included 53 visits to the 8 landfills (denoted as landfills A–H) on 19 days (19 May 2021 through 1 July 2021, 19 deployments in 44 days). To accommodate other MOOSE sampling objectives, visits did not use fixed schedules, rather, most sampling was conducted along predetermined routes with varying start and end times. The "south loop" included visits to five landfills (A–F), all located west and southwest of Detroit, and required about 5 h to complete. The "north loop" visited three landfills (D, G, H), all located north of Detroit, and required about 6 h. Most (17 of 19 days) of Phase 1 measurements were conducted in late morning or mid-day when boundary layer heights tended to be high, which typically decreases CH_4 levels from landfill emissions (as noted later). Phase 2 was designed to measure CH_4 levels while the boundary layer height was low and included 13 visits in the early morning on 9 sampling days at four landfills, and 1 visit to a landfill in the evening on a 10th day (all between 19 July 2021 through 29 September 2021, 10 deployments in 72 days). The Phase 2 schedule permitted only one or two landfills to be visited per day. Each landfill was visited on multiple occasions, and the number of visits to the landfills across both study phases ranged from 4 to 16. In most cases, the sampling date, time and the landfill(s) visited were determined to meet other MOOSE sampling objectives. Data acquired covered the hours from 6:00 to 20:00. Since MOOSE was focused on the regional ozone and its precursor monitoring, all field work was conducted from early summer to early fall, thus seasonal variation was not examined.

During each visit, MPAL was driven along the perimeter of the landfill completing at least one loop and was parked at a downwind location on the perimeter loop for at least 5 min to collect stationary data (the vehicle was parked facing the landfill to reduce the likelihood of self-pollution, if feasible). Public roads were used. (We were not permitted to enter the landfills.) In Phase 2, most visits included four loops around the landfill, and downwind transects were collected for distances of 1.6–3.2 km (1–2 miles) on selected days. As shown later, the sizes of the 8 landfills varied, but the perimeter loop was typically 5 km in length and required 15–30 min to complete.

Sampling protocols for MPAL are detailed elsewhere [29]. No sample handling was needed. Two calibrations, one prior to the sampling campaign (17 May 2021), and one after 13 deployments (21 June 2021), were performed at the Michigan Department of Environment, Great Lakes, and Energy (EGLE) facility.

2.2. Data Collection

Pollutant data were collected by MPAL, a truck-based platform that contains five lab-quality gaseous pollutant instruments, five particulate matter (PM) instruments, meteorological sensors, a geographical positioning sensor (GPS), and forward and reverse cameras. In 2021, MPAL was temporarily adapted into a smaller vehicle without the PM instruments; otherwise the instruments, power, and data acquisition systems were unchanged as noted elsewhere [29]. CH_4 measurements were obtained using two cavity ring-down spectrometers (Models G2204 and G2401, Picarro, Santa Clara, CA, USA) that have 0–100 ppm range, 0.001 ppm resolution, and 2 s time resolution. In addition to CH_4, the G2204 instrument measures H_2S and H_2O, and the G2401 measures CO, CO_2 and H_2O. These two instruments had separate sampling inlets: the G2401 sampled from a roof-top inlet above the vehicle at ~2.5 m height; the G2204 sampled using an array of six vertical, downward-facing sampling ports evenly distributed across the front bumper at ~10 cm height above the road. Details of the design and operation of the inlet systems can be found elsewhere [29]. MPAL acquired location and meteorological data simultaneously with the pollutant measurements. A high-speed GPS (Garmin 18x, Garmin International Inc., Olathe, KS, USA) recorded location data (uncertainty generally under 3 m), and vehicle speed and direction. Ambient temperature, relative humidity (RH), wind speed and wind direction were measured by a meteorological system (Model 92000, R.M. Young Company, Traverse City, MI, USA) installed on a short mast (0.7 m) above the vehicle roof. Wind measurements were corrected for vehicle speed and direction. All data were collected by using MPAL's data acquisition system at 1 Hz.

Quality assurance protocols included regular zero and span checks, continuous monitoring of sample flows, temperatures, sampling and reactor pressures, and post-hoc reviews to ensure concentration (and other parameters) were in acceptable ranges. We adjusted measurements for the lag times resulting from instrument response and the sampling inlet system. CH_4 concentrations measured from the roof and front bumper inlets were compared using scatter plots and descriptive statistics.

We collected information on a number of environmental conditions that can affect LFG emissions and ambient concentrations. Surface meteorological data from four airport sites in the region (Detroit Metro Wayne County Airport (DTW), Grosse Ile Municipal Airport, Detroit City Airport, and Willow Run Airport) were acquired to supplement the MPAL meteorological data [30]. Data across the airport sites were averaged to obtain hourly values of wind speed (m/s) and direction, temperature (°C), barometric pressure (mbar) and ceiling height (m); these data can be more representative than MPAL's on-board meteorological sensors, which can be affected by local surroundings (vehicles, trees, buildings) as well as vehicle speed and direction changes. Wind roses were generated with eight directions and four wind speed bins (0–2, 2–4, 4–6, >6 m/s) using an online program (WRPLOT View Version 8.0.2) [31]. Because decreases in barometric pressure can draw subsurface LFG into the atmosphere [32], we estimated the barometric pressure change in time, ΔP (mbar/h), by smoothing the local barometric pressure (averaged across from the four airports) using 24-h running averages, and then taking 6 and 24 h differences per hour to obtain ΔP_{6h} and ΔP_{24h}. Landfill temperature affects the rate of microbial methanogenesis and CH_4 emissions [33]. Two estimates of soil temperatures (°C) were obtained. First, we smoothed hourly airport temperatures using 1-week running averages, and then used lags of 0, 30, 60, and 90 days ($T_{air,0}$, $T_{air,30}$ $T_{air,60}$ $T_{air,90}$), reflecting the time lag needed to transfer heat from the surface to deeper soils where methanogenesis occurs. Second, we obtained records of soil temperatures at 10 cm depth available from a nearby site (22 km from Landfill C; latitude/longitude: 42.5982/−83.4964) from the Michigan Automated Weather Network and Environ-weather program [34]; these temperatures also were lagged by 0, 30, 60, and 90 days ($T_{soil,0}$, $T_{soil,30}$ $T_{soil,60}$ $T_{soil,90}$), again to reflect deeper layers of the landfill. LFG releases to the atmosphere will disperse to the height of the boundary layer. Hourly estimates of boundary layer height (H in m) at each landfill, for the date and time of each visit, were extracted from the GEM-MACH model [35–37]. Occasionally, this model predicted very low heights; these low values were increased to 100 m and referred to as the adjusted boundary layer height H_{adj}.

Information pertaining to landfill characteristics was obtained from the annual reports published by the State of Michigan [38]. This included the annual volume of municipal and commercial waste (MCW) disposed at each landfill from 2012–2021, from which 5- and 10-year total disposal volumes were calculated.

2.3. Data Analysis and Modeling

After validation, we consolidated the 1-s data collected by MPAL into a master dataset containing the timestamp, vehicle location and speed, meteorological parameters, CH_4 levels measured by both instruments, and other pollutant data. Procedures for data validation and consolidation are described elsewhere [29]. We checked for possible outliers in the 1-s CH_4 data by comparing high percentile concentrations measurements (e.g., 95th, 99th, and 99.9th percentile) for each visit and identifying large gaps. To further confirm the representativeness of the CH_4 data, and to show the effect of using instrumentation with slower response times in landfill surveys, we calculated statistics of peak CH_4 levels using 5 to 60 s block averages computed from the 1-s data.

Data analyses included descriptive statistics, measures of daily and diurnal variation in CH_4 levels, and comparisons among sites. Maps displaying CH_4 levels were generated for the landfill visits using nonlinear bins (cut points of 0, 1.9, 2.0, 2.2, 2.4, 2.6, 3.0, 5.0, 10.0 ppm) that better indicated locations or zones with elevated levels than linear scales. Daily maps illustrated measurements obtained on each day (1–4 loops) at each landfill, and composite maps averaged across measurements on different days. Wind roses were constructed for the dates and times of visits to each landfill to visualize the influence of surface winds on CH_4 peak locations. We investigated relationships between CH_4 levels and landfill size, using annual records of disposal volumes over the past 10 years.

Time-of-day analyses were performed at landfill C, which had the most (16) visits that spanned a wide range of hours throughout the day (06:00 to 21:00). Data at this site was also used to investigate the relationship between CH_4 levels measured at landfill C and environmental conditions. Initially, single variables were linearly regressed against CH_4 levels, including H, u, P, ΔP_{6h}, ΔP_{24h}, and soil temperatures (including surrogates) at different lags (e.g., $T_{air,0}$, $T_{air,30}$, $T_{air,60}$, $T_{air,90}$, $T_{soil,0}$, $T_{soil,30}$ $T_{soil,60}$, $T_{soil,90}$). Given the expected inverse relationship between concentrations with wind speed and boundary layer height, we also regressed 1/u and 1/H against CH_4 levels. Scatterplots were used to visualize results. These analyses used both the daily average and maximum CH_4 levels measured across the multiple loops obtained on different sampling days. Then, the joint effects of variables on CH_4 levels were investigated using multivariate models, both with and without interactions terms (e.g., 1/(H u), P/H). Variables selected in these models were based on results of single variable analyses, e.g., using the landfill temperature or surrogate that achieved the highest fit. All combinations of meteorological variables were tested with interaction terms, however, the number of interaction terms was limited to two in order to avoid over-fitting. Model parameters were estimated using bootstrap analyses, 1500 times resampling and the boot() and boot.ci() functions in R-Studio [39,40]. Calculated statistics included model coefficients, standard errors, r^2, and nonparametric 95% confidence intervals determined using accelerated confidence intervals (BCa), which are asymptotically better than other estimates [41]. We confirmed that model parameters fitted using gradient search methods were comparable. These multivariate models were fit to the average, median, 90th percentile and maximum CH_4 measurements on different days.

We also evaluated the use of a physically-based dilution-type model to fit the daily maxima CH_4 measurements found along the landfill perimeter roads. This model considered the landfill as the sole emission source that dispersed into a fully mixed regime defined by the boundary layer height H and ground surface (see the SI Equations S1–S3 for more description):

$$C \propto Q(Hu)^{-1} \tag{1}$$

where C = daily maximum CH_4 concentration (ppm), Q = CH_4 emission rate (kg/s), H = boundary layer height (m), and u = wind speed (m/s). The dependence of emission rates on landfill temperature T (°C), barometric pressure P (mbar), or temporal pressure change ΔP (mbar/h) was incorporated using linear models that lead to a final model:

$$C = B_5 + \frac{B_6(B_3 + P)(B_4 + T)}{(B_1 + H)(B_2 + u)} \tag{2}$$

where B_1–B_6 are fitted parameters. Parameters of Equation (2) were estimated using a generalized gradient search that minimized the total squared error.

3. Results and Discussion

3.1. Data Review

Over the 29 sampling days in Phases 1 and 2, a total of 169,067 1-s measurements were collected at the eight landfills, representing 47 h of sampling while driving a total of 1083 km at an average speed of 23.1 km/h. This dataset excludes transit to the landfills, i.e., only driving along perimeter roads and short distances to measure downwind gradients are included.

The outlier analysis (Table S1) showed no obvious outliers in the dataset, thus warranting the use of 1-s data. Increasing the CH_4 averaging time from 1 s to 5 s reduced the maximum concentrations observed at the landfills by 0 to 9%, depending on the landfill; longer averaging periods led to greater decreases, e.g., 10, 20 and 60 s averaging periods led to decreases of 1–24, 2–28, and 11–50% (Table S2). The effect of averaging time depends on a number of factors, including the size and orientation of the CH_4 plume, driving speed, and instrumentation (the instruments used provide measurements at 1 Hz, but their true response time is ~2 s). Our results suggest that acceptable performance (e.g., within 25% of true value) might be obtained using less expensive instrumentation that has a response time not longer than 20 s in mobile monitoring applications at landfills if a low driving speed (<25 km/h) is maintained. However, this response time and vehicle speed limits the ability to localize a source to a 139 m segment (response time × speed). Generally, high frequency instruments are desirable for mobile platforms given typically faster vehicle speeds, narrow plumes or otherwise localized concentration "hotspots."

Overall median and average CH_4 levels during the 66 landfill visits were 2.33 and 3.94 ppm, respectively (Table 1), which exceeded general ambient levels (1.9–2.2 ppm) [42]. Elevated CH_4 levels were detected at all eight landfills, and the maximum (1 s) concentration at the eight landfills varied from 4.49 to 37.58 ppm.

Table 1. Summary of CH_4 levels at eight landfills. Phase 1 visits did not have a designated visit time. Most phase 2 visits were conducted in the early morning. Ranges of daily 90th percentile and maximum concentrations in parentheses.

Landfill	No. of Visits	Average (ppm)	SD (ppm)	Min (ppm)	Median (ppm)	75th Percentile (ppm)	90th Percentile (ppm)	Max (ppm)	Sampling Time (min)
Phase 1: 05/19–07/01/2021									
A	9	2.21	0.50	1.91	2.01	2.17	2.78 (2.06–3.62)	5.71 (2.19–5.71)	362
B	9	2.89	1.47	1.91	2.12	3.17	5.30 (2.05–6.26)	10.57 (2.63–10.57)	318
C	11	2.62	1.29	1.89	2.04	2.56	4.14 (2.07–6.64)	12.26 (2.25–12.26)	165
D	6	2.20	0.44	1.94	2.04	2.21	2.63 (2.11–3.56)	7.45 (2.72–7.45)	95
E	4	2.22	0.28	1.96	2.15	2.25	2.61 (2.25–2.77)	3.97 (2.50–3.97)	70
F	4	2.09	0.21	1.96	2.04	2.11	2.18 (1.98–2.23)	4.49 (2.25–4.49)	93
G	5	2.25	0.60	1.89	1.98	2.18	3.36 (1.95–3.95)	4.69 (2.26–4.69)	83
H	5	2.03	0.33	1.89	1.96	2.00	2.12 (2.06–3.18)	4.61 (2.26–4.61)	67
Phase 2: 07/19–09/29/2021									
A	3	2.76	1.53	2.00	2.16	2.65	4.13 (3.52–4.53)	16.02 (8.07–16.02)	331
B	3	5.18	4.54	2.02	2.97	7.28	11.04 (2.18–12.65)	37.58 (7.51–37.58)	152
C	5	5.35	4.36	1.99	3.47	6.30	11.49 (5.05–16.35)	36.38 (8.81–36.38)	731
D	2	6.98	6.62	2.00	3.35	10.21	18.35 (3.90–19.07)	29.69 (6.32–29.69)	350
Overall	66	3.94	3.89	1.89	2.33	3.68	8.19 (1.95–19.07)	37.58 (2.19–37.58)	2818

3.2. Roof-Top Versus Front Bumper Measurements

The simultaneous roof-top and front bumper CH_4 measurements were highly correlated (r^2 = 0.97; Figure S2), and most pairs of observations (when concentration differences were <5 ppm) fitted a 1:1 line. However, a small subset of measurements (0.38% of all data) had differences exceeding 5 ppm. Of these, 57% had higher front bumper measurements and 43% had higher roof-top measurements, and nearly all (98%) cases occurred at landfills B, C and D in Phase 2 (2% occurred at landfill A in Phase 1). These large differences could result from several factors, e.g., highly localized ground level releases, elevated plumes from flare stacks and other combustion sources, very low boundary layer heights and/or localized circulation patterns such as cold air drainage in conjunction with localized releases, instrument faults, misaligned instrument responses, and different instrument response times. Because these differences occurred at a small set of locations and on multiple occasions (Figure S3), and the same disagreements occurred with 5-s averaged data (attenuated by <15%), we tend to rule out instrument faults and alignment issues (although these cannot be entirely eliminated). Using trend plots, we identified that a contributing factor was the difference in response times as the roof-top measurements had a faster response than the front bumper measurements (Figure S4). This difference, which may be attributable to the design of the front bumper inlet (using an array of sampling ports) and its longer sampling line, as well as instrument differences, would tend to decrease the levels of very short peaks. (Note that a relatively high flow was maintained in the sampling lines, and that we corrected for travel time within the sampling line.)

The largest concentration difference occurred near the NE corner of landfill B where roof-top measurements were as much as 29 ppm higher than the simultaneous ground level measurement. At this landfill, concentration differences always had higher roof-top peaks. This location was adjacent to a large but closed landfill immediately to the north that together with landfill B formed a valley running E-W; additionally, many of the concentration differences occurred relatively close (~50 m) from a small compressor station on the closed landfill. No other nearby elevated CH_4 sources were identified, although the faces of both the open and closed landfills are well above road grade. Given the light traffic at this location (an occasional garbage truck and few other vehicles; Figure S3), traffic-related emissions were highly unlikely to cause repeated measurement differences. The opposite situation–ground level CH_4 measurements that exceeded rooftop measurements–occurred predominantly at landfill D. While the landfill rises well above the road level, some gas collection lines, bore holes, sampling wells, well-heads and a new landfill cell were close to the north perimeter road. Releases from such facilities could produce the observed CH_4 concentration gradient under meteorological conditions that limit dispersion, e.g., very low boundary layer heights (100–400 m on 5 August 2021) and low wind speed (1.3 m/s on 5 August 2021), conditions when most measurement differences were detected).

We saw little evidence that nearby combustion sources caused the CH_4 measurement differences in this study. Flaring and flare stacks were observed only on the north side of landfill A, the east side of landfill B, the NE corner of the closed landfill near landfill B, and the north side of landfill D. Only the flare stacks at landfill D were close to the sites of the measurement differences, although no flaring was observed during our visits. For operating flares or other combustion sources, elevated levels of NO_2, CO_2 and other combustion pollutants would be expected. In this study, no obvious NO_2 and CO_2 elevations were identified that accompanied disagreed CH_4 measurements.

In summary, sampling height did not affect the vast majority of CH_4 measurements, and thus, subsequent analyses in this study use the roof inlet measurements since they had higher time resolution, may be more representative, better captured elevated plumes, and since data availability was higher (due to downtime caused by repairs of the ground level inlet instrument). We note that simultaneous measurements of CH_4, CO_2 and NO_2 may help distinguish fugitive sources (releasing only LFG) from combustion sources such as (operating) flares, engines, and turbines (releasing both CH_4 and combustion products).

3.3. Daily Variation and Landfill Comparisons

The number of visits and CH_4 measurements at each landfill are summarized in Table 1. Mid-day phase 1 concentration statistics are displayed in Figure 1. The average, minimum and median CH_4 levels were similar and close to background levels (1.9–2.2 ppm), and even the 75th percentile levels at seven of the eight landfills did not show meaningful site impacts. The exception, landfill B, more frequently showed elevated levels, possibly due to the relatively short distance (~300 m) between the perimeter road and the active landfill face. However, the 90th percentile and above levels were elevated at all landfills, and a maximum concentration of 12.3 ppm was reached at landfill C during phase 1. CH_4 levels in Phase 2, which were mostly morning measurements, were more elevated and the maximum levels reached 37.6 and 36.4 ppm at landfill B and C, respectively. The visit-to-visit variation in the daily 90th percentile and maximum concentrations was notable, especially in Phase 1 when even maximum concentrations on some visits to landfills A, F, G and H did not substantially exceed background levels (Table 1). Thus, mid-day perimeter sampling may not always indicate CH_4 releases. In contrast, sampling in phase 2 always showed elevated levels, including the 50th percentile level (55th percentile at landfill A). This shows the need to sample under certain meteorological conditions to show site impacts, as explored later.

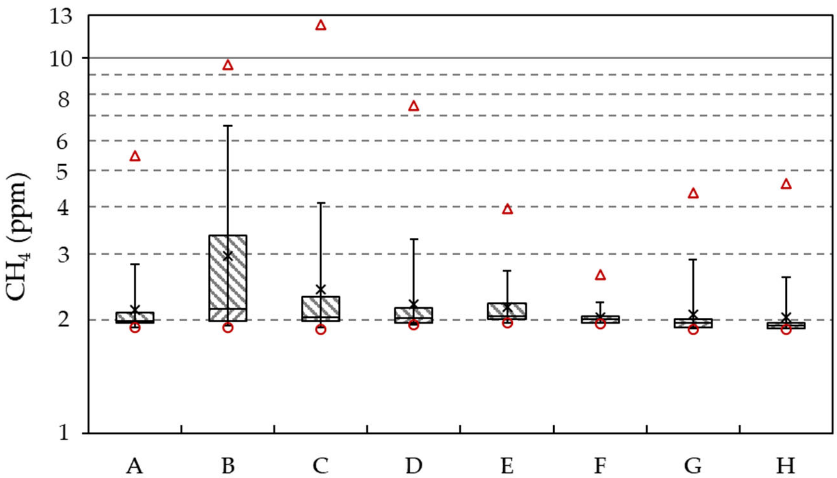

Figure 1. Statistics of CH_4 levels acquired during mid-day (11:00–17:00) in Phase 1 at the eight landfills. The boxes represent the 25th, median, and 75th percentiles; bars represent the 5th and 95th percentiles; cross, triangle and circle represent average, maximum and minimum representatively.

Maps showing CH_4 levels around the eight landfills are shown in Figure 2. Daily maps showing each visit to the landfills are shown in Figures 3 and S5–S9. CH_4 levels tended to approach background levels at most locations, however, "hotspots" with higher CH_4 levels often occurred at one or several perimeter locations, suggesting either localized releases or a broad plume from the landfill. Most hotspots were located in the downwind direction of the landfill, as illustrated by the daily maps. For example, Figure 3 shows peaks in the downwind direction of landfill C on most sampling days, except on 7 June 2021 when levels along the east road and SW corner suggest releases near the sampling location. Visits on 19 May 2021, 2 June 2021 and 9 June 2021, which had similar sampling times and wind conditions, showed sizable differences, e.g., the peak on 19 May 2021 was wider and CH_4 levels were higher, possibly due to the low boundary layer height (<100 m according to the GEM-MACH model). Maps for 19 July 2021, 20 July 2021 and 3 August 2021 had peaks at the southwest corner that did not correspond to the wind direction, again suggesting ground-level releases (discussed in Section 3.1). Phase 2 maps (Figures 3 and S5–S9 dated after 7 January 2021) differ in that CH_4 concentrations were at least slightly elevated (>2.2 ppm) along much of the landfill perimeter, suggesting effects of low boundary layer heights, low wind speeds, and possibly the overnight build-up of CH_4.

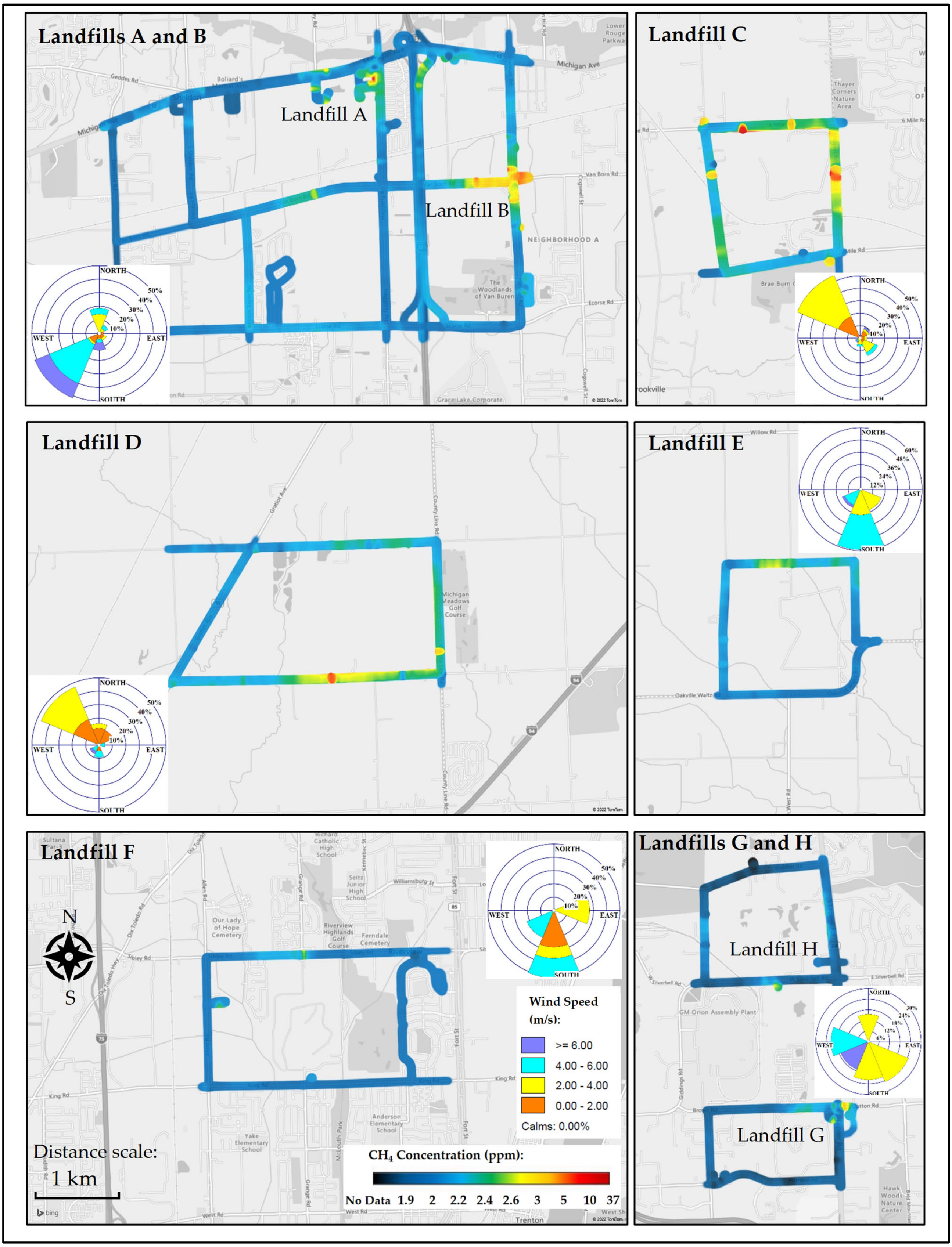

Figure 2. Composite maps showing average CH_4 concentrations around the eight landfills (Landfill A to Landfill H) over all visits in Phases 1 and 2. Inset wind rose shows direction and speed of surface winds during the sampling period at each landfill.

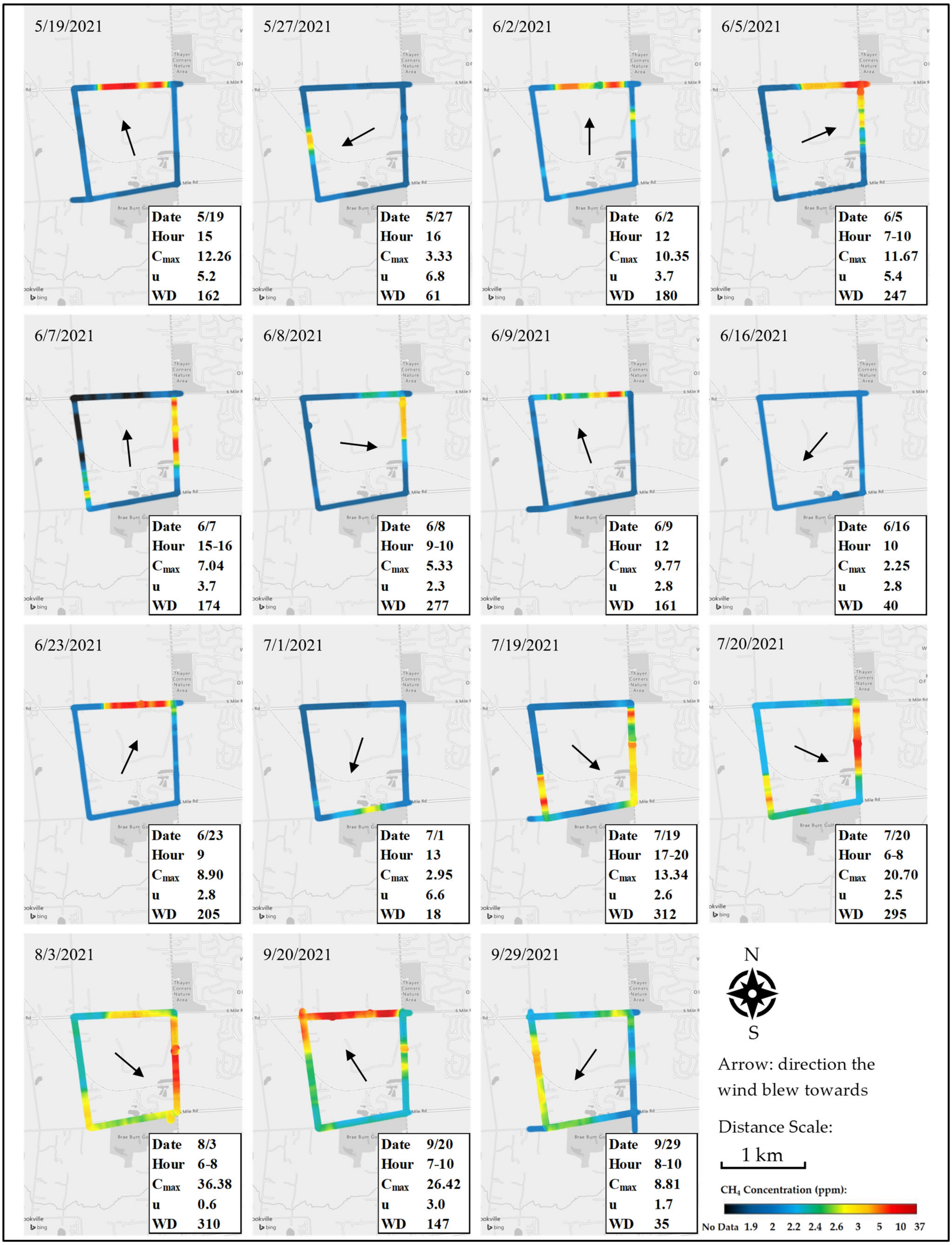

Figure 3. Daily maps showing CH_4 concentrations at landfill C. Figures are titled by the visit date in the format month/day/year. The arrow indicates the dominant wind direction. Inset boxes show sampling date, hour, maximum concentration (C_{max}, ppm), wind speed (u, m/s) and dominant wind direction (WD).

Landfill emissions and measured CH_4 levels can be influenced by many factors. These include landfill size; integrity and performance of the landfill cover, cap and gas collection system; waste characteristics including composition and age; landfill conditions affecting the rate of methanogenesis (e.g., temperature, moisture); meteorological conditions affecting dispersion in ambient air and vapor migration in the landfill; topography; and the distance between emission sources and measurement locations (i.e., perimeter road). We next examine several of these factors.

The eight landfills vary in size, shape and elevation, as indicated by Figure 2. Most rise to considerable height above the largely flat surrounding terrain (seven landfills have a relief of 50–70 m; landfill H has a 30 m relief [43]). This topography may induce effects on winds, e.g., air drainage and terrain steering, which shifts peak locations under some conditions.

The CH_4 generation rate at a landfill is dependent on disposal volumes, which are plotted in Figure 4 for each landfill over the past ten years. Since 2019, landfills B, C, D and E received considerably more waste (total of 2.5–7.0 million cubic yards/year) than landfills A, F, G, and H (0.5–1.4 million cubic yards/year). Across the landfills, CH_4 concentrations tended to be higher at landfills receiving a larger cumulative waste volume, as shown in Figure 5, which plots the maximum CH_4 measurements at the landfill versus the landfills' waste volume. The mid-day CH_4 measurements (11:00 to 17:00) in phase 1 are used in this analysis, during which all eight landfills were visited; these measurements help to minimize effects from highly variable mixing conditions. The highest correlation (r^2 = 0.32) between current CH_4 levels and waste volume occurred for waste volumes over the 2012–2016 period, representing aged waste (Figure 5a). Some of the highest CH_4 measurements were obtained at landfills B, C and D, which disposed of the largest volumes of waste (23 to 51 million cubic yards over the past 10 years); landfill E had large quantities (33 million cubic yards) but lower concentrations, possibly because the perimeter road was relatively far from the landfill face. CH_4 levels were low at landfills A, F, G and H, which had smaller waste volumes. The moderately strong association between waste volume and CH_4 levels is surprising given that the analysis did not incorporate meteorological or other factors that can affect emissions and ambient concentrations.

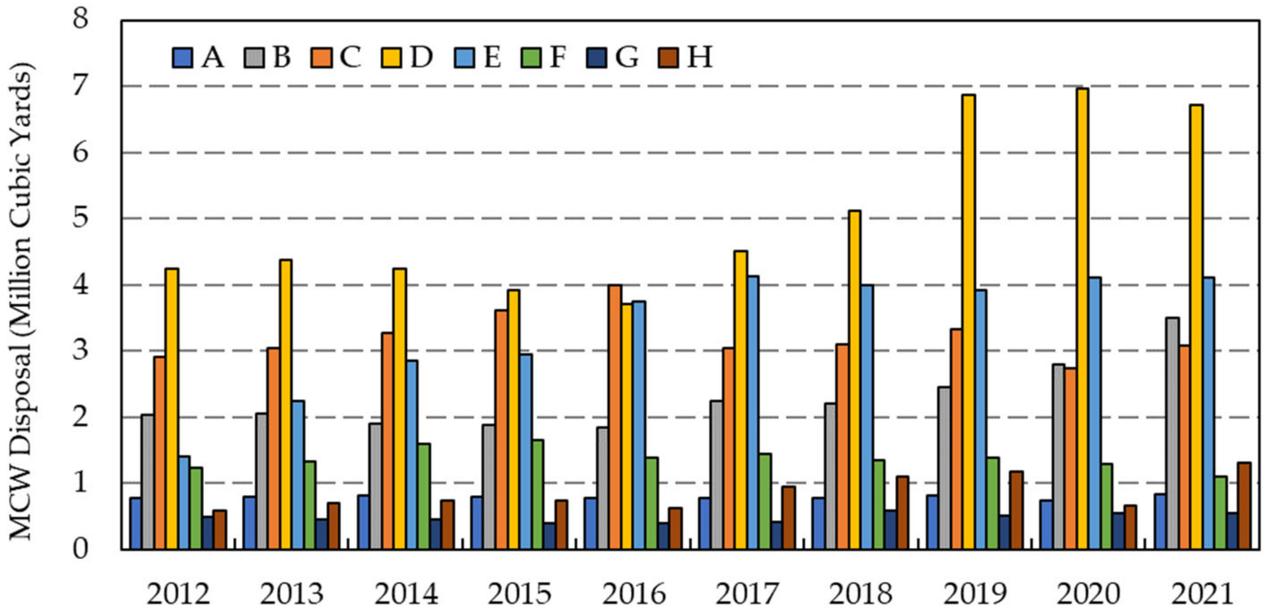

Figure 4. Annual MCW disposal volumes at the eight landfills for years 2012 through 2021.

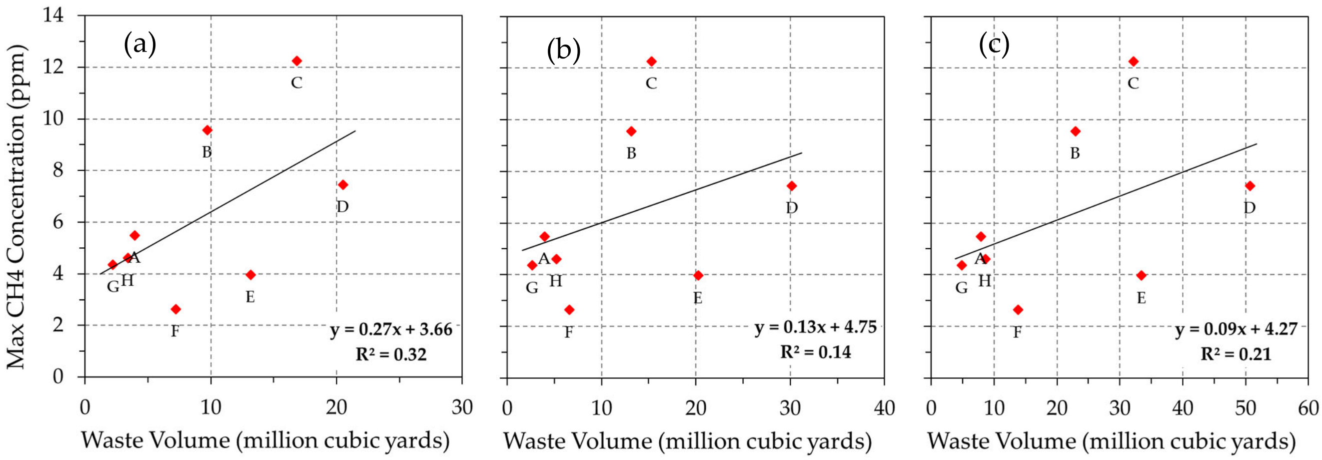

Figure 5. Plots of maximum CH_4 levels versus cumulative waste volumes at the eight landfills (indicated as A–H) for three periods: (**a**) 2012–2016; (**b**) 2017–2021; and (**c**) 2012–2021. Regression line and r^2 are shown for each plot. Waste volumes are period totals.

3.4. Diurnal Variations

The diurnal variation in CH_4 levels was evaluated at landfill C, which was visited most frequently (16 visits) with visit durations from 10 to 120 min (total 15 h) on 15 sampling days between 6:00 and 21:00. Average CH_4 levels and meteorological conditions during these visits by time of day are shown in Figure 6. Northerly to easterly winds dominated the sampling periods. Median, 90th percentile and maximum CH_4 concentrations were highest in the early morning (before 10:00 am) and increased in the evening (after 17:00; Figure 6a), likely due to relatively stagnant conditions on site associated with low wind speeds and low boundary layer heights. Barometric pressure remained relatively constant by time-of-day and no direct effect on CH_4 levels was expected or observed (Figure 6b). Trends in Figure 6 suggest an inverse relationship between CH_4 levels and wind speed and boundary layer height, as portrayed in Equation (1); Section 3.5 provides a quantitative analysis using both multivariate and dilution models.

While suggesting strong trends, the analysis of diurnal variability is limited by several factors. First, the analysis is based on a limited number of visits. A longer record would better characterize meteorological parameters, e.g., we noted only small changes in barometric pressure through the study. Second, meteorological parameters were measured at airports some distance from the landfills. Third, the boundary layer estimates had large uncertainties (shown by error bars in Figure 6d) due to day-to-day variation and uncertainty in the GEM-MACH model estimates. Finally, this analysis does not account for the multiple influences, as explored in the next section. The strong diurnal variability in CH_4 levels at landfills does highlight the benefit that continuous and real-time CH_4 monitoring at landfills could provide.

3.5. Univariate and Multivariate Models for CH_4 Levels

Models using a single meteorological parameter to fit landfill C CH_4 measurements are presented in Table 2. Models with the highest fit (based on r^2 for the daily maximum CH_4 concentration) used the inverse of wind speed (r^2 = 0.532; 95% CI: 0.009–0.952), and the "best" model for the daily average CH_4 concentration used the 30-day lagged soil temperature (r^2 = 0.539: 95% CI: 0.242–0.823), although models using 30-day lags for air temperature (T_{air}) achieved nearly comparable r^2 (0.503). The 6 h temporal pressure change ΔP_{6h} attained r^2 of 0.113 and 0.184 for the daily average and maximum, respectively. Models utilizing $1/H$ and $1/H_{adj}$ had only weak correlation ($r^2 < 0.1$). Except for soil temperature, r^2 values were higher when fitting daily maximum CH_4 compared to the daily average. This may result since meteorological parameters such as wind speed, temporal pressure change, and boundary layer height affect the dispersion of CH_4 emissions, while soil temperature governs the methanogenesis activity in the landfills, affecting CH_4 level across the landfill site. Overall, Table 2 shows the strongest (and expected) inverse relationships with wind speed u and boundary layer height H (without adjustment); CH_4 levels also showed strong and direct relationships with soil temperature $T_{soil,30}$ and barometric pressure difference ΔP_{6h}. These four variables were selected for the multivariate models.

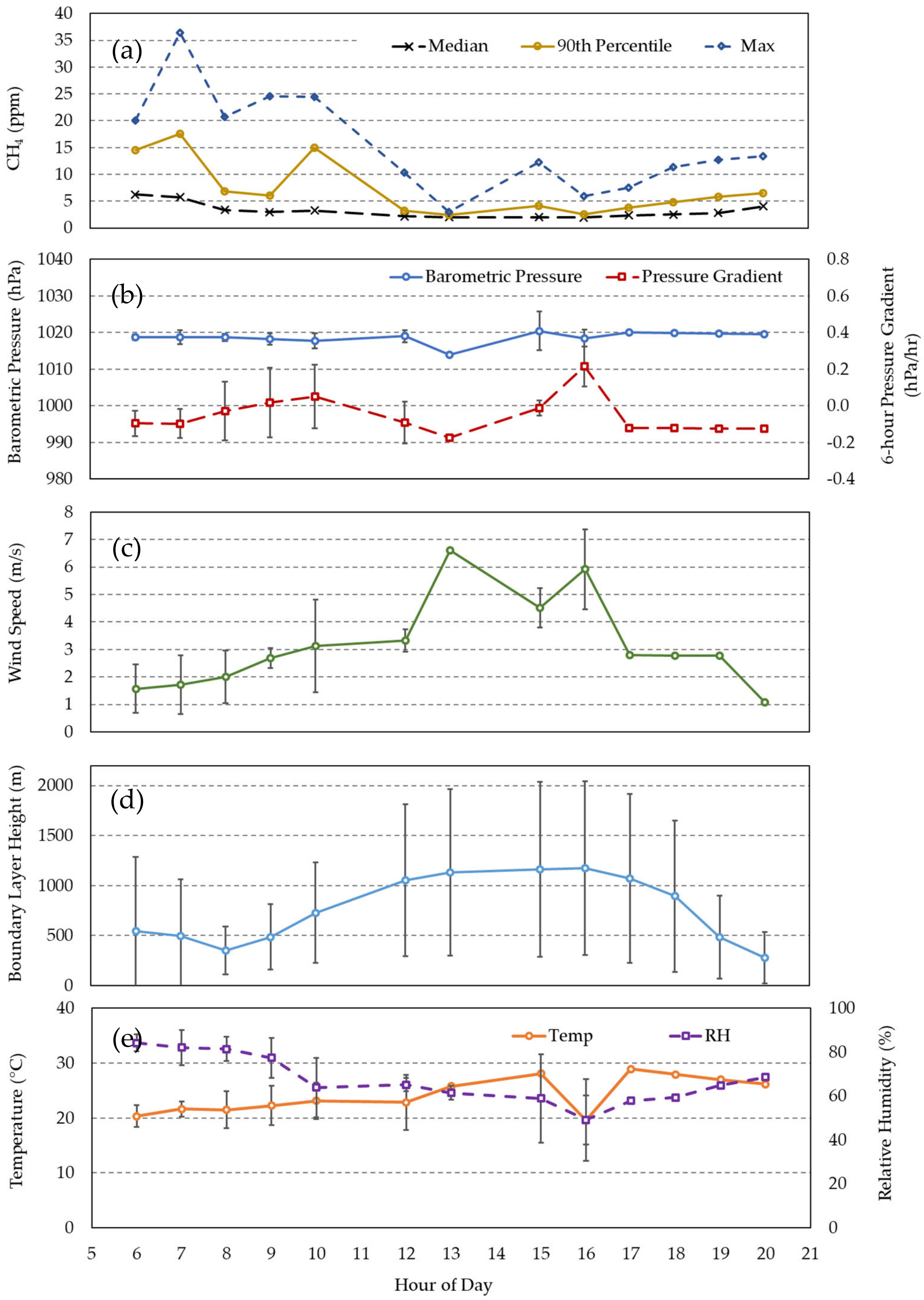

Figure 6. Diurnal variation of CH_4 concentrations and hourly average of meteorological variables: (**a**) CH_4 concentration statistics; (**b**) barometric pressure and pressure change; (**c**) wind speed; (**d**) modeled boundary layer height; and (**e**) I temperature and relative humidity (RH) at landfill C. Error bars show the range over 15 visits.

Table 2. Results of single variable analyses using a linear model (Equation (1)). The inverse of boundary layer height and wind speed were examined. H_{adj} is maximum of H and 100 m. Heat map indicates magnitude of r^2.

Variable	CH4 Level	Intercept	Slope	r^2	Bca 95% CI
1/H	Daily Ave	3.71	−4.37	0.083	(0.0002, 0.2143)
	Daily Max	13.20	−25.64	0.094	(0.0007, 0.4219)
$1/H_{adj}$	Daily Ave	3.16	55.02	0.016	(0.0000, 0.1910)
	Daily Max	8.98	485.40	0.041	(0.0002, 0.3438)
1/u	Daily Ave	2.32	2.87	0.428	(0.0312, 0.9586)
	Daily Max	4.74	17.63	0.532	(0.0089, 0.9523)
P	Daily Ave	−107.52	0.11	0.041	(0.0001, 0.3596)
	Daily Max	−925.68	0.92	0.097	(0.0013, 0.3487)
ΔP_{6h}	Daily Ave	3.54	−3.58	0.113	(0.0003, 0.4695)
	Daily Max	12.29	−25.07	0.184	(0.0006, 0.5905)
ΔP_{24h}	Daily Ave	3.55	−1.12	0.012	(0.0000, 0.1125)
	Daily Max	12.51	−11.40	0.040	(0.0000, 0.3968)
$T_{air,0}$	Daily Ave	2.83	0.03	0.004	(0.0000, 0.0554)
	Daily Max	10.83	0.05	0.000	(0.0000, 0.0010)
$T_{air,30}$	Daily Ave	0.13	0.20	0.503	(0.2034, 0.7554)
	Daily Max	−3.14	0.91	0.335	(0.3973, 0.6770)
$T_{air,60}$	Daily Ave	1.63	0.14	0.253	(0.0339, 0.6030)
	Daily Max	4.12	0.59	0.148	(0.0495, 0.5327)
$T_{air,90}$	Daily Ave	2.66	0.12	0.351	(0.0652, 0.7732)
	Daily Max	8.57	0.49	0.191	(0.0778, 0.8329)
$T_{soil,0}$	Daily Ave	0.79	0.13	0.045	(0.0000, 0.3052)
	Daily Max	−3.66	0.76	0.049	(0.0001, 0.2939)
$T_{soil,30}$	Daily Ave	−0.06	0.22	0.539	(0.2419, 0.8227)
	Daily Max	−4.12	1.00	0.364	(0.4370, 0.5823)
$T_{soil,60}$	Daily Ave	0.95	0.20	0.435	(0.1241, 0.7658)
	Daily Max	0.19	0.91	0.308	(0.3003, 0.5763)
$T_{soil,90}$	Daily Ave	2.47	0.15	0.341	(0.0505, 0.7292)
	Daily Max	7.67	0.61	0.198	(0.0952, 0.6862)

Table 3 shows five multivariate models applied for the daily maximum concentrations selected from the full list of models estimated. (Table S3 shows all models, including models fitting the average, 98th and 99th percentile, and maximum CH_4 concentrations.) As seen earlier, models for the daily maximum concentration achieved the highest r^2. Models 1 and 2 use additive terms with 3 and 4 meteorological variables, respectively, and achieved r^2 above 0.73. Models 4, 5 and 6 added two interaction terms. This increased the r^2 to 0.88 in model 5 which used 7 fitted parameters for the intercept, 1/H, 1/u, ΔP_{6h}, $T_{soil,30}$, and interaction terms 1/(H u), and ΔP_{6h}/u.

Table 3. Selected multivariate models (models 1–5) and the fitted dilution model (model 6).

Model	Equation	R^2
(1)	$C_{max} = 5.88 - \frac{14.34}{H} + \frac{17.24}{u} - 21.96\Delta P_{6h}$	0.73
(2)	$C_{max} = 1.90 - \frac{12.32}{H} + \frac{15.23}{u} - 19.64\Delta P_{6h} + 0.29\ T_{soil,30}$	0.75
(3)	$C_{max} = -0.79 + \frac{127.96}{H} + \frac{21.07}{u} - 18.32\Delta P_{6h} + 0.32\ T_{soil,30} - \frac{405.01}{Hu}$	0.77
(4)	$C_{max} = -1.94 + \frac{49.46}{H} + \frac{14.26}{u} - 15.49\Delta P_{6h} + 0.48\ T_{soil,30} - \frac{385.99\Delta P_{6h}}{H}$	0.78
(5)	$C_{max} = -5.18 + \frac{203.74}{H} + \frac{19.88}{u} + 29.14\Delta P_{6h} + 0.62\ T_{soil,30} - \frac{611.79}{Hu} - \frac{144.21\Delta P_{6h}}{u}$	0.88
(6)	$C_{max} = 5.6 - \frac{11044.6(\Delta P_{6h} - 0.3)(T_{soil,30} - 6.9)}{(991.9 + H)(1.0 + u)}$	0.89

The fitted dilution model, shown in Table 3 as model 6, attained a slightly higher fit (r^2 = 0.89) than the multivariate models using 6 fitted parameters. This model attained a mean squared error (MSE) of 9.18 ppm^2. Model performance is plotted in Figure 7a and compared to two of the multivariate models (Figure 7b,c). While attaining the highest r^2 and closely fitting the highest CH_4 levels, the dilution model poorly predicted levels below 10–15 ppb; multivariate model 5 provided slightly better performance in this regime although higher concentrations were not as closely predicted. Modifications might be made to the multivariate models to improve predictions during daytime periods (e.g., 10:00 to 17:00) when the boundary layer height and wind speed increased sharply and likely became the controlling variables. The supplemental materials present separate models for daytime measurements in which removing the temporal pressure change and soil temperature terms increases the r^2 from 0.02 to 0.35 for C_{max} < 10 ppm (Equation (S4) and Figure S10). These models indicate that boundary layer height, wind speed, temporal pressure change, and soil temperature are determinants of CH_4 levels at landfills. However, because a relatively small dataset was used to estimate up to 7 parameters in these models, confidence interval for the r^2 values is wide. (Estimates of the 95th confidence intervals for the r^2 were typically 0.30 to 0.94 for models 1-5 using bootstrap analyses, and 0.83–0.94 for model 6 using F-distribution [44]).

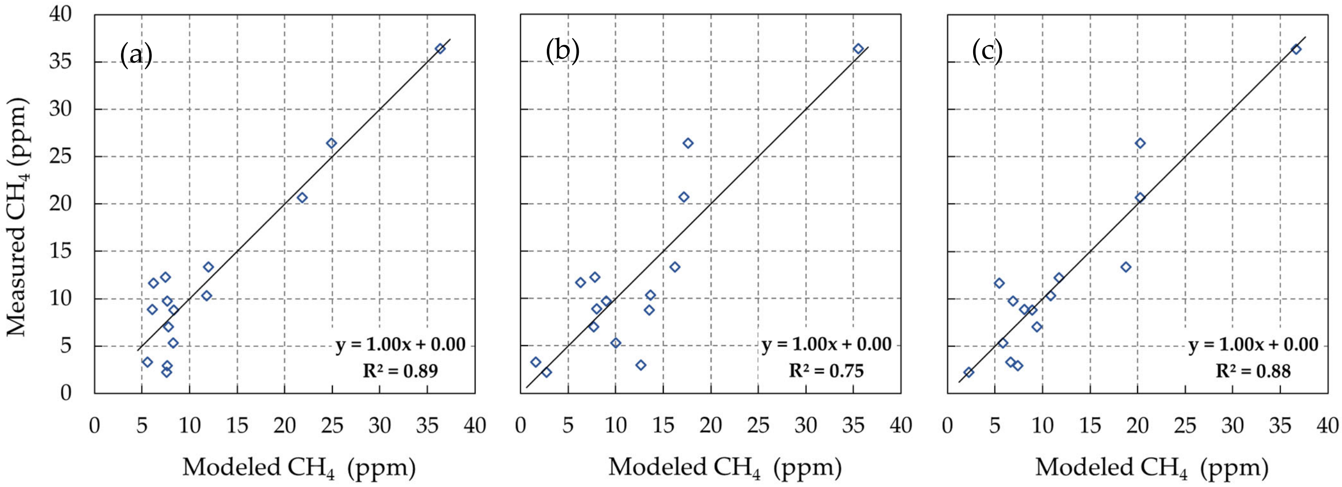

Figure 7. Scatter plots of measured CH_4 daily maximum concentrations versus modeled values: (**a**) uses dilution model (model 6); (**b**) uses 4 parameter additive model (model 2); and (**c**) uses 4 parameter model with 2 interaction terms (model 5).

3.6. Discussion

We have demonstrated the feasibility of using mobile monitoring to characterize CH_4 levels around landfills, including diurnal, daily and spatial variation. On mid-day visits, we detected mostly small, localized and low concentration peaks at perimeter roads around the eight landfills, probably due to rapid dispersion of LFG emissions and, in some cases, elevated plumes from sources such as flares and pipe leaks. Higher CH_4 levels were found during stagnant atmospheric conditions, e.g., in early morning, and levels were elevated along large portions of the perimeter roads and not necessarily only in the downwind direction. The highest CH_4 concentration detected was 37.6 ppm. Somewhat comparable results were obtained at a landfill in north-central Texas, which showed localized peaks and a maximum concentration of 54.8 ppm [25]. However, four studies using mobile measurements reported only very low CH_4 concentrations, generally below 3 ppm and close to background levels of 2 ppm. These studies used measurements 1–5 km downwind of the landfill that were coupled with tracer gas measurements in order to estimate CH_4 emissions [45–48].

Mønster et al. illustrated that the wind direction could change the location and shape of concentration peaks near a landfill [47]. While concentration measurements are affected by winds, boundary layer height, dispersion rates, source locations and geometry, mobile monitoring allows rapid and repeated measurements that can detect "hotspots" that may require additional monitoring and mitigation. Additionally, it can provide the repeated measurements needed to characterize spatial and temporal variability, important for designing monitoring programs and interpreting results. Although less accurate than tracer gas correlation techniques, mobile monitoring data can be used with atmospheric dispersion models to estimate locations and rates of CH_4 leaks at landfills [49]. This process requires accurate local wind measurements, detailed landfill topography and near-source measurements inside the landfill, which were not available in this study.

Landfills are large and heterogenous emission sources. Soil temperature affects LFG production rates on a seasonal basis, and barometric pressure fluctuations and failures of LFG collection and treatment systems can affect emission rates on an hourly to daily basis. We found that the disposed volume of aged waste (particularly over 5–10 years earlier) was positively correlated to CH_4 levels. This differs from a Columbian study which reported 4-fold higher biochemical methane potential (BMP) for fresh waste as compared to 5-year aged waste [50]. The disagreement may be due to different climate conditions (tropical in Colombia vs. temperate continental in Michigan, USA) and different waste composition since waste in developing countries typically contains a much larger proportion of organic waste, mainly food wastes that degrade fast [51]. While LFG production rates may be relatively stable, fugitive releases may be intermittent and episodic, tied to leaks, system failures and upsets (e.g., malfunctioning flares). Our data suggests most CH_4 releases at landfills result from fugitive and not combustion sources.

In addition to emission variability, atmospheric concentrations depended strongly on wind speed and boundary layer height. We found that the multivariate and dilution-type models using four meteorological factors (boundary layer height, wind speed, temporal barometric pressure change and soil temperature) yielded a strong correlation with observed CH_4 levels. Both types of models obtained comparable performance, at least when the multivariate models included several interaction terms including $\Delta P_{6h}/u$ and $1/(H\ u)$. The dilution model had less agreement if the maximum CH_4 concentrations were below 10–15 ppm, which usually occurred during daytime (10:00 to 17:00) when the boundary layer height and wind speed increased sharply and likely became the controlling variables. Other types of models or parametrizations might address these discrepancies. Additional data from landfill visits that cover the full range of meteorological conditions and seasons are suggested.

We recognize several limitations of the data. While we monitored wind direction and speed at 1-s intervals on the MPAL, these data were not necessarily reliable given the vehicle movements, low sampling height (~2.5 m), nearby trees, and other factors that can affect winds. Instead, we used hourly data from nearby airports, which ranged 20–45 km from the landfill. Mixing height data reported at airports were unreliable, and replaced with modeled boundary layer heights, which introduced other uncertainties. We did not obtain measurements in winter when snow and ice cover and meteorological changes might significantly alter results. However, the measurements collected should be representative of conditions during the summer ozone season. Landfill temperatures were unavailable, and thus we used 10 cm soil temperature data from a site 22 km distant with a 30-day lag to estimate soil temperature deeper in the landfill. Such measures are approximate and do not account for internal heat production in the landfill. To address such shortcomings and obtain more representative data, meteorological and soil parameters ideally would be monitored on site. We also recognize limitations regarding the simple dilution model, which assumes a flat landfill surface, homogeneous winds, and fully mixed conditions. It does not incorporate terrain features, vertical air movement, distance to the actual release points and landfill geometry, soil moisture (which promotes CH_4 generation [52]), and other factors. As noted earlier, perimeter monitoring of atmospheric CH_4 levels does not capture the vertical profile of CH_4 concentrations needed to quantity fluxes and emission rates. Lastly, we studied only large, active and elevated landfills that may not be representative of smaller landfills, closed landfills, or subgrade configurations (e.g., using quarries).

Despite some limitations, the present study provides valuable information to guide future on-site measurements and mobile monitoring strategies. Concentration maps generated using mobile monitoring can help to identify leaks and can screen and identify areas where CH_4 levels are frequently elevated. Fixed-site continuous monitors might be deployed at these locations to capture emission events and estimate emission rates. The diurnal analyses suggest the best times for mobile platforms deployments, e.g., early morning, and the relationship to levels measured later in the day. Sampling and modeling results demonstrate the dependence of ambient CH_4 levels at landfills on wind speed, wind direction and boundary layer height, thus on-site meteorological measurements are recommended.

4. Conclusions

Mobile measurements repeatedly collected along perimeter roads at eight large and operating landfills in southeast Michigan showed elevated CH_4 concentrations, often along one side or corner of a landfill, predominantly determined by the wind direction. The maximum CH_4 levels reached 38 ppm, well above typical background levels of 2 ppm. Pollutant mapping showed that locations with elevated levels tended to be consistent across visits, although the concentrations were highly variable. In most cases, CH_4 measurements obtained with the near surface (10 cm) and elevated (2.5 m) inlets were essentially identical. We also found that averaging times for the CH_4 measurements from 1 to 20 s yielded similar distributions, suggesting that lower speed measurements using simpler and less expensive instrumentation could perform well in landfill applications.

CH_4 concentrations were related to the size of the landfill, as measured by waste volume, and the highest correlation was found for the cumulate waste volumes from 5 to 10 years earlier, suggesting that several years may be required before methanogenic degradation of the waste is maximized. The highest CH_4 levels occurred in the early morning when winds were light, and the estimated boundary layer height was low, consistent with the dispersion potential for a local source. Conversely, mid-day sampling was likely to produce "false negatives", i.e., no meaningful elevation in CH_4 levels above background levels. We also correlated CH_4 levels to the temporal barometric pressure change, consistent with pressure driven fluxes of LFG, and to surrogates of soil or landfill temperature, consistent with rates of methanogenesis. Both the mechanistically-based dilution and multivariate models incorporating a small set of meteorological variables explained a high fraction (up to 89%) of the variability in CH_4 levels at the landfill visited most frequently.

The present study has several limitations. MPAL was deployed to landfills on only 29 days, and relatively few mornings and no night-time visits were completed. The relatively small dataset limits opportunities for model validation and did not permit an analysis of seasonal variation. On-site meteorological and soil parameters were not available, and the estimates from distant stations introduced uncertainties. Factors such as terrain features, vertical air movement, site geometry and distance to the release points, and soil moisture, were not incorporated.

Several recommendations are made to improve the future characterization of CH_4 releases at landfills using mobile platforms. Because much of the variation in CH_4 levels results from meteorological factors, on-site measurements of wind speed, direction and boundary layer height are recommended. As it is impractical to utilize mobile monitoring for continuous measurements, we recommend using continuous real-time CH_4 monitoring at one or several fixed sites in the prevailing downwind areas to supplement mobile measurements and better characterize temporal variability. Mobile and fixed site sampling schedules should capture diurnal and seasonal patterns using consistent sampling approaches and a minimum of 1-year of measurements. This larger dataset will improve the reliability of spatial-temporal modeling of CH_4 levels and emissions, as well as capture transients and localized hotspots that can help identify and locate leaks and other anomalies. Predictive models might incorporate additional parameters, including CH_4 levels inside the landfill, CH_4 profiles above the landfill, ambient temperature, precipitation, landfill moisture, snow cover, and waste type and volume. Finally, these and the perimeter measurements as collected in this study can be utilized in inverse dispersion models to estimate CH_4 emissions from landfills [23].

Supplementary Materials: The following supporting information can be downloaded at: https://www.mdpi.com/article/10.3390/atmos14060906/s1, Development of a dilution model; Figure S1: Map of eight visited landfills, four airport meteorological stations, and major CH4 sources in southeast Michigan; Figure S2: Comparison between the roof and front bumper inlet CH4 measurements; Figure S3: Locations where the roof and front bumper inlet measurements showed >5 ppm difference; Figure S4: Trend plots of the five CH4 peaks with the largest roof-top and near-ground measurement differences; Figure S5: Maps of daily CH4 concentration measured at Landfills A and B; Figure S6: Maps of daily CH4 concentration measured at Landfill D; Figure S7: Maps of daily CH4 concentration measured at Landfill E; Figure S8: Maps of daily CH4 concentration measured at Landfill F; Figure S9: Maps of daily CH4 concentration measured at Landfills G and H; Figure S10: Scatter plots of measured CH4 daily maximum concentrations (<10 ppm) against the modeled value calculated with (a) Model 6 and (b). Equation S1: dilution of emissions into a fully mixed layer extending between the ground level and the boundary layer height H (m); Equation S2: Cbaseline is the CH4 baseline concentration; Equation S3: the influence of several factors on the average emission rate Q; Equation S4: optimized by the GRG nonlinear method; Table S1: Visit date, time, number of observations and average, standard deviation (SD) and top CH4 concentration percentiles (in ppm) at Landfill C.; Table S2: Maximum CH4 concentrations (in ppm) measured at each landfill at different averaging times; Table S3: Results for the multivariate models.

Author Contributions: Conceptualization, S.A.B.; Methodology, T.X., S.G.B., C.A.S. and S.A.B.; Software, T.X., S.G.B. and S.A.B.; Validation, T.X., J.R., S.G.B. and S.A.B.; Formal Analysis, T.X. and S.G.B.; Investigation, T.X., S.G.B. and S.A.B.; Resources, S.A.B.; Data Curation, T.X., J.R. and C.A.S.; Writing—Original Draft Preparation, T.X. and S.G.B.; Writing—Review and Editing, S.A.B.; Visualization, T.X.; Supervision, S.A.B.; Project Administration, S.A.B.; Funding Acquisition, S.A.B. All authors have read and agreed to the published version of the manuscript.

Funding: Funding supporting this research was obtained from the State of Michigan in grant 00E02952/AQDGG2020P2 provided by the U.S. Environmental Protection Agency (EPA) entitled "The Southeast Michigan Chemical Source Signature (CHESS) Experiment". Additional support was provided by grants P30ES017885 and R01ES032389 from the National Institute of Environmental Health Sciences, National Institutes of Health. The content is solely the responsibility of the authors and does not necessarily represent the official views of the sponsors.

Institutional Review Board Statement: Not applicable.

Informed Consent Statement: Not applicable.

Data Availability Statement: Related data for this study and other components of MOOSE can be found at: https://www-air.larc.nasa.gov/missions/moose/index.html (accessed on 1 April 2023).

Acknowledgments: We appreciate the assistance of our laboratory and field staff, including Chris Godwin, Maxine Coady and Nelson Figueroa. We also acknowledge the support of Eduardo P. Olaguer, Shelley Jeltema, Susan Kilmer, Navnit Ghuman, and Eric Hansen at the Michigan Department of Environment, Great Lakes and Energy.

Conflicts of Interest: The authors declare no conflict of interest.

References

1. Stocker, T.F.; Qin, D.; Plattner, G.K.; Tignor, M.; Allen, S.K.; Boschung, J.; Nauels, A.; Xia, Y.; Bex, V.; Midgley, P.M. *Climate Change 2013: The Physical Science Basis. Intergovernmental Panel on Climate Change, Working Group I Contribution to the IPCC Fifth Assessment Report (AR5)*; IPCC: Geneva, Switzerland, 2013.
2. Fiore, A.M.; Jacob, D.J.; Field, B.D.; Streets, D.G.; Fernandes, S.D.; Jang, C. Linking Ozone Pollution and Climate Change: The Case for Controlling Methane. *Geophys. Res. Lett.* **2002**, *29*, 25-1–25-4. [CrossRef]
3. West, J.J.; Fiore, A.M. Management of Tropospheric Ozone by Reducing Methane Emissions. *Environ. Sci. Technol.* **2005**, *39*, 4685–4691. [CrossRef] [PubMed]
4. West, J.J.; Fiore, A.M.; Horowitz, L.W.; Mauzerall, D.L. Global Health Benefits of Mitigating Ozone Pollution with Methane Emission Controls. *Proc. Natl. Acad. Sci. USA* **2006**, *103*, 3988–3993. [CrossRef] [PubMed]

5. Yusuf, R.O.; Noor, Z.Z.; Abba, A.H.; Hassan, M.A.A.; Din, M.F.M. Methane Emission by Sectors: A Comprehensive Review of Emission Sources and Mitigation Methods. *Renew. Sustain. Energy Rev.* **2012**, *16*, 5059–5070. [CrossRef]
6. US EPA Organization. Basic Information about Landfill Gas. Available online: https://www.epa.gov/lmop/basic-information-about-landfill-gas (accessed on 21 September 2022).
7. Maasakkers, J.D.; Jacob, D.J.; Sulprizio, M.P.; Turner, A.J.; Weitz, M.; Wirth, T.; Hight, C.; DeFigueiredo, M.; Desai, M.; Schmeltz, R.; et al. Gridded National Inventory of U.S. Methane Emissions. *Environ. Sci. Technol.* **2016**, *50*, 13123–13133. [CrossRef]
8. US EPA Organization. Draft Inventory of U.S. Greenhouse Gas Emissions and Sinks: 1990–2021. Available online: https://www.epa.gov/ghgemissions/draft-inventory-us-greenhouse-gas-emissions-and-sinks-1990-2021 (accessed on 29 March 2023).
9. Lan, X.; Thoning, K.W.; Dlugokencky, E.J. Trends in Globally-Averaged CH_4, N_2O, and SF_6 Determined from NOAA Global Monitoring Laboratory Measurements. Version 2023-04. Available online: https://doi.org/10.15138/P8XG-AA10 (accessed on 12 December 2022) [CrossRef]
10. U.S. EPA Regulatory Impact Analysis of the Supplemental Proposal for the Standards of Performance for New, Reconstructed, and Modified Sources and Emissions Guidelines for Existing Sources: Oil and Natural Gas Sector Climate Review. Available online: https://www.epa.gov/system/files/documents/2022-12/Supplemental-proposal-ria-oil-and-gas-nsps-eg-climate-review-updated.pdf (accessed on 12 March 2023).
11. US EPA Organization. Municipal Solid Waste Landfills: New Source Performance Standards (NSPS), Emission Guidelines (EG) and Compliance Times. Available online: https://www.epa.gov/stationary-sources-air-pollution/municipal-solid-waste-landfills-new-source-performance-standards (accessed on 22 December 2022).
12. ATSDR—Landfill Gas Primer—Chapter 2: Landfill Gas Basics. Available online: https://www.atsdr.cdc.gov/hac/landfill/html/ch2.html (accessed on 21 September 2022).
13. Powell, J.T.; Townsend, T.G.; Zimmerman, J.B. Estimates of Solid Waste Disposal Rates and Reduction Targets for Landfill Gas Emissions. *Nat. Clim. Chang.* **2016**, *6*, 162–165. [CrossRef]
14. Mønster, J.; Kjeldsen, P.; Scheutz, C. Methodologies for Measuring Fugitive Methane Emissions from Landfills—A Review. *Waste Manag.* **2019**, *87*, 835–859. [CrossRef]
15. Babilotte, A.; Lagier, T.; Fiani, E.; Taramini, V. Fugitive Methane Emissions from Landfills: Field Comparison of Five Methods on a French Landfill. *J. Environ. Eng.* **2010**, *136*, 777–784. [CrossRef]
16. MethaneSAT. Available online: https://www.methanesat.org/ (accessed on 23 February 2023).
17. O'Keefe, A.; Deacon, D.A. Cavity Ring-down Optical Spectrometer for Absorption Measurements Using Pulsed Laser Sources. *Rev. Sci. Instrum.* **1988**, *59*, 2544–2551. [CrossRef]
18. Hanson, R.K.; Varghese, P.L.; Schoenung, S.M.; Falcone, P.K. *Absorption Spectroscopy of Combustion Gases Using a Tunable IR Diode Laser*; ACS Publications: Washington, DC, USA, 1980; ISBN 1947-5918.
19. Shaw, J.T.; Shah, A.; Yong, H.; Allen, G. Methods for Quantifying Methane Emissions Using Unmanned Aerial Vehicles: A Review. *Philos. Trans. R. Soc. Math. Phys. Eng. Sci.* **2021**, *379*, 20200450. [CrossRef] [PubMed]
20. Kim, Y.M.; Park, M.H.; Jeong, S.; Lee, K.H.; Kim, J.Y. Evaluation of Error Inducing Factors in Unmanned Aerial Vehicle Mounted Detector to Measure Fugitive Methane from Solid Waste Landfill. *Waste Manag.* **2021**, *124*, 368–376. [CrossRef] [PubMed]
21. Shah, A.; Allen, G.; Pitt, J.R.; Ricketts, H.; Williams, P.I.; Helmore, J.; Finlayson, A.; Robinson, R.; Kabbabe, K.; Hollingsworth, P.; et al. A Near-Field Gaussian Plume Inversion Flux Quantification Method, Applied to Unmanned Aerial Vehicle Sampling. *Atmosphere* **2019**, *10*, 396. [CrossRef]
22. MOOSE—Michigan-Ontario Ozone Source Experiment. Available online: https://www-air.larc.nasa.gov/missions/moose/ (accessed on 22 December 2022).
23. Olaguer, E.P.; Jeltema, S.; Gauthier, T.; Jermalowicz, D.; Ostaszewski, A.; Batterman, S.; Xia, T.; Raneses, J.; Kovalchick, M.; Miller, S.; et al. Landfill Emissions of Methane Inferred from Unmanned Aerial Vehicle and Mobile Ground Measurements. *Atmosphere* **2022**, *13*, 983. [CrossRef]
24. Zazzeri, G.; Lowry, D.; Fisher, R.E.; France, J.L.; Lanoisellé, M.; Nisbet, E.G. Plume Mapping and Isotopic Characterisation of Anthropogenic Methane Sources. *Atmos. Environ.* **2015**, *110*, 151–162. [CrossRef]
25. Lan, X.; Talbot, R.; Laine, P.; Torres, A. Characterizing Fugitive Methane Emissions in the Barnett Shale Area Using a Mobile Laboratory. *Environ. Sci. Technol.* **2015**, *49*, 8139–8146. [CrossRef]
26. Ars, S.; Vogel, F.; Arrowsmith, C.; Heerah, S.; Knuckey, E.; Lavoie, J.; Lee, C.; Pak, N.M.; Phillips, J.L.; Wunch, D. Investigation of the Spatial Distribution of Methane Sources in the Greater Toronto Area Using Mobile Gas Monitoring Systems. *Environ. Sci. Technol.* **2020**, *54*, 15671–15679. [CrossRef]
27. Land of Waste: American Landfills by State. Available online: https://www.visualcapitalist.com/sp/land-of-waste-american-landfills-by-state/ (accessed on 23 February 2023).
28. US EPA Organization. 2017 National Emissions Inventory (NEI) Data. Available online: https://www.epa.gov/air-emissions-inventories/2017-national-emissions-inventory-nei-data (accessed on 7 May 2023).
29. Xia, T.; Catalan, J.; Hu, C.; Batterman, S. Development of a Mobile Platform for Monitoring Gaseous, Particulate, and Greenhouse Gas (GHG) Pollutants. *Environ. Monit. Assess.* **2021**, *193*, 7. [CrossRef]
30. Team, N.G. Hourly/Sub-Hourly Observational Data. Available online: https://www.ncei.noaa.gov/maps/ (accessed on 22 February 2022).

31. Lakes EnvironWRPLOT View. Lakes Environ. Softw. Available online: https://www.weblakes.com/software/freeware/wrplot-view/#:~:text=WRPLOT%20View%20is%20a%20fully,for%20several%20meteorological%20data%20formats (accessed on 21 March 2023).
32. Czepiel, P.M.; Shorter, J.H.; Mosher, B.; Allwine, E.; McManus, J.B.; Harriss, R.C.; Kolb, C.E.; Lamb, B.K. The Influence of Atmospheric Pressure on Landfill Methane Emissions. *Waste Manag.* **2003**, *23*, 593–598. [CrossRef]
33. Chen, H.; Zhu, T.; Li, B.; Fang, C.; Nie, M. The Thermal Response of Soil Microbial Methanogenesis Decreases in Magnitude with Changing Temperature. *Nat. Commun.* **2020**, *11*, 5733. [CrossRef]
34. Michigan Automated Weather Network. Available online: https://mawn.geo.msu.edu/ (accessed on 26 January 2023).
35. Whaley, C.H.; Galarneau, E.; Makar, P.A.; Akingunola, A.; Gong, W.; Gravel, S.; Moran, M.D.; Stroud, C.; Zhang, J.; Zheng, Q. GEM-MACH-PAH (Rev2488): A New High-Resolution Chemical Transport Model for North American Polycyclic Aromatic Hydrocarbons and Benzene. *Geosci. Model Dev.* **2018**, *11*, 2609–2632. [CrossRef]
36. Ren, S.; Stroud, C.A.; Belair, S.; Leroyer, S.; Munoz-Alpizar, R.; Moran, M.D.; Zhang, J.; Akingunola, A.; Makar, P.A. Impact of Urbanization on the Predictions of Urban Meteorology and Air Pollutants over Four Major North American Cities. *Atmosphere* **2020**, *11*, 969. [CrossRef]
37. Stroud, C.A.; Ren, S.; Zhang, J.; Moran, M.D.; Akingunola, A.; Makar, P.A.; Munoz-Alpizar, R.; Leroyer, S.; Bélair, S.; Sills, D.; et al. Chemical Analysis of Surface-Level Ozone Exceedances during the 2015 Pan American Games. *Atmosphere* **2020**, *11*, 572. [CrossRef]
38. Annual Reports of Solid Waste Landfilled in Michigan. Available online: https://www.michigan.gov/egle/about/organization/materials-management/solid-waste/solid-waste-disposal-areas/annual-reports-of-solid-waste-landfilled-in-michigan (accessed on 4 November 2022).
39. Canty, A.; Ripley, B.D. *Boot: Bootstrap R (S-Plus) Functions*, R package version 1.3-28.1; R Core Team: Indianapolis, IN, USA, 2022.
40. Davison, A.C.; Hinkley, D.V. *Bootstrap Methods and Their Applications*; Cambridge University Press: Cambridge, UK, 1997; ISBN 0-521-57391-2.
41. Canty, A.J. Resampling Methods in R: The Boot Package. *Newsl. R Proj. Vol.* **2002**, *2*, 2–7.
42. Xia, T.; Raneses, J.; Batterman, S. Improving the Performance of Pipeline Leak Detection Algorithms for the Mobile Monitoring of Methane Leaks. *Atmosphere* **2022**, *13*, 1043. [CrossRef]
43. 3D Maps and Peaks Identification. Available online: https://peakvisor.com/ (accessed on 29 March 2023).
44. Leontyev, A. Confidence Intervals for R-Squared. Available online: https://agleontyev.netlify.app/post/2019-09-05-calculating-r-squared-confidence-intervals/ (accessed on 8 May 2023).
45. Jakober, C.A.; Mara, S.L.; Hsu, Y.-K.; Herner, J.D. Mobile Measurements of Climate Forcing Agents: Application to Methane Emissions from Landfill and Natural Gas Compression. *J. Air Waste Manag. Assoc.* **2015**, *65*, 404–412. [CrossRef] [PubMed]
46. Mosher, B.W.; Czepiel, P.M.; Harriss, R.C.; Shorter, J.H.; Kolb, C.E.; McManus, J.B.; Allwine, E.; Lamb, B.K. Methane Emissions at Nine Landfill Sites in the Northeastern United States. *Environ. Sci. Technol.* **1999**, *33*, 2088–2094. [CrossRef]
47. Mønster, J.; Samuelsson, J.; Kjeldsen, P.; Scheutz, C. Quantification of Methane Emissions from 15 Danish Landfills Using the Mobile Tracer Dispersion Method. *Waste Manag.* **2015**, *35*, 177–186. [CrossRef]
48. Foster-Wittig, T.A.; Thoma, E.D.; Green, R.B.; Hater, G.R.; Swan, N.D.; Chanton, J.P. Development of a Mobile Tracer Correlation Method for Assessment of Air Emissions from Landfills and Other Area Sources. *Atmos. Environ.* **2015**, *102*, 323–330. [CrossRef]
49. Bel Hadj Ali, N.; Abichou, T.; Green, R. Comparing Estimates of Fugitive Landfill Methane Emissions Using Inverse Plume Modeling Obtained with Surface Emission Monitoring (SEM), Drone Emission Monitoring (DEM), and Downwind Plume Emission Monitoring (DWPEM). *J. Air Waste Manag. Assoc.* **2020**, *70*, 410–424. [CrossRef]
50. Sandoval-Cobo, J.J.; Casallas-Ojeda, M.R.; Carabalí-Orejuela, L.; Muñoz-Chávez, A.; Caicedo-Concha, D.M.; Marmolejo-Rebellón, L.F.; Torres-Lozada, P. Methane Potential and Degradation Kinetics of Fresh and Excavated Municipal Solid Waste from a Tropical Landfill in Colombia. *Sustain. Environ. Res.* **2020**, *30*, 7. [CrossRef]
51. Caicedo-Concha, D.M.; Sandoval-Cobo, J.J.; Fernando, C.-Q.R.; Marmolejo-Rebellón, L.F.; Torres-Lozada, P.; Sonia, H. The Potential of Methane Production Using Aged Landfill Waste in Developing Countries: A Case of Study in Colombia. *Cogent Eng.* **2019**, *6*, 1664862. [CrossRef]
52. Rasapoor, M.; Young, B.; Brar, R.; Baroutian, S. Enhancement of Landfill Gas Generation from Aged Waste by a Combination of Moisture Adjustment and Application of Biochar and Neutral Red Additives: A Field-Scale Study. *Fuel* **2021**, *283*, 118932. [CrossRef]